Advances in Military Technology
Vol. 20, No. 1, 2025, pp. 123-135
ISSN 1802-2308, eISSN 2533-4123
DOI 10.3849/aimt.01921

Influence of Double Cone Liner Shape on Jet Characteristics of Shaped Charge

P. Konečný*, P. Skalický and T. Anh Hoang

Department of Weapon and Ammunition, University of Defence, Brno, Czech Republic

The manuscript was received on 24 September 2024 and was accepted after revision for publication as an original research paper on 22 April 2025.

Abstract:

This article deals with a simulation of the influence of double cone liner shape on the jet characteristics of a small-sized shaped charge by ANSYS AUTODYN software. The results prove that, with a smaller apex angle, a smaller base angle, and a larger distance from the top of the liner to the transition position of the cone angle, the jet velocity and jet length will be larger. For a 40 mm shaped charge used in the study, a double cone liner with shape parameters including an apex angle of 40°, a base angle of 60°, and a cone angle transition position from the top of the liner at a value equal to 0.3 times, the base diameter is predicted to provide the best jet performance. The research results are the basis for evaluating the influence of liner shape on the jet formation process and designing a double cone liner for small-sized shaped charges.

Keywords:

shaped charge, double cone liner, jet characteristics, apex angle, base angle

1 Introduction

Shaped charges are extensively utilized in military equipment because of the jet penetrating power, which enables them to effectively breach armored targets, destroy fortifications, and create precision openings in various structures. The structure of the jet is shown in Fig. 1. With an appropriate stand-off distance, the penetration efficiency of the jet increases when it has a very high jet tip velocity and the difference in velocity between the tip and tail of the jet (rules of changing in jet velocity) is greater [1].

There are many methods to increase the jet tip velocity and the jet efficiency, such as using explosives with high detonation velocity and high compression ability [1-4] or improving the structure of the shaped charge [5]. Incorporating a wave shaper

* *Corresponding author: Department of Weapon and Ammunition, University of Defence, Kounicova 156/65, CZ-662 10 Brno, Czech Republic. Phone: +420 973 442 037, E-mail: pavel.konecny@unob.cz. ORCID 0000-0003-0703-2315.*

into the structure of the shaped charge is another solution to enhance jet characteristics [6, 7], however, for small-sized shaped charges, there is insufficient space to arrange a wave shaper. Some studies have investigated the use of high-density liner materials such as tungsten and molybdenum, as mentioned in [8], as well as metals like silver, zirconium, titanium, and depleted uranium [9], or tungsten-copper alloys [10]. These studies have shown that jets formed from these metals exhibit higher tip velocities and longer jet lengths compared to copper liners. However, due to the economics and popularity of the materials, these metals are difficult to use in liner production. Solutions that involve altering the geometrical properties of the liner, such as using a liner with variable thickness [11, 12], or using a multilayered liner [13], have also proven effective in improving jet performance.

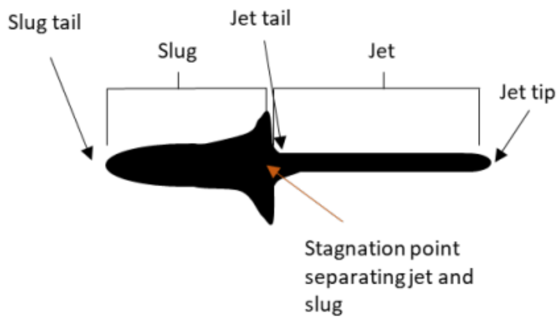

Fig. 1 The structure of the jet [14]

One of the simple, yet highly effective methods is to alter the shape of the liner. Liners with different shapes can generate varying jet characteristics [1]. Some commonly applied liner shapes include conical, tapered conical, hemispherical, tulip, and trumpet shapes.

The trumpet liner (with a length-to-base diameter ratio of the liner larger than 1.3) has the smallest apex angle and the largest base angle. Hence, the velocity difference between the tip and tail of the jet is larger, leading to a large jet elongation and a larger jet length compared to other types of liners. The advantages of trumpet liners in improving jet performance have also been demonstrated in [15, 16]. However, the disadvantage of the trumpet liner is that it requires complex manufacturing technology and poor stability [17]. To overcome this drawback, a double cone liner is used in practical applications which takes advantage of the power of the trumpet liner while ensuring technological factors in the production process.

Fig. 2 shows the dimensions of a double cone liner. The liner apex angle is $2\alpha_1$, the base angle is $2\alpha_2$, and the cone angle transition position from the top of the liner is h_1. D is the diameter of the cone base, h is the length of the liner, δ is the wall thickness of the liner, and r is the inner circle radius on the top of the liner.

The numerical simulation is performed using ANSYS AUTODYN software, which can be used to solve nonlinear problems related to impact, penetration, perforation, and explosion and has built-in mathematical models such as shaped charge jetting analysis. AUTODYN hydrocode is based on mass, momentum, and energy conservation equations, where the materials can be defined by its equation of state and its strength model [18].

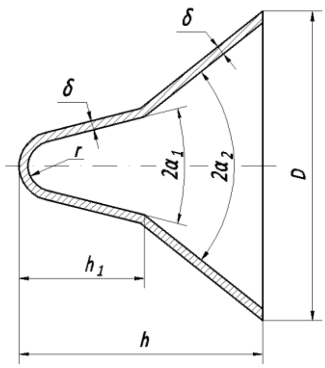

Fig. 2 Dimensions of the double cone liner

In this paper, the numerical simulation method on ANSYS AUTODYN software (2024 R1) is used to study the jet characteristics of a small-caliber shaped charge using a double cone liner. The effects of the parameters of the apex cone angle, base cone angle, and cone angle transition position were analyzed, providing a research foundation for the design of a double cone liner.

2 Simulation Model

This section presents a method of building simulation models using ANSYS AUTODYN 2D software.

2.1 Description of the Simulation

Fig. 3 introduces the simulation model on ANSYS AUTODYN 2D software. The shaped charge model used in the study was designed based on the shaped charge of the 40 mm HE-DP92 projectile which has a diameter of 40 mm, a length of 38 mm, and a charge diameter of 36 mm.

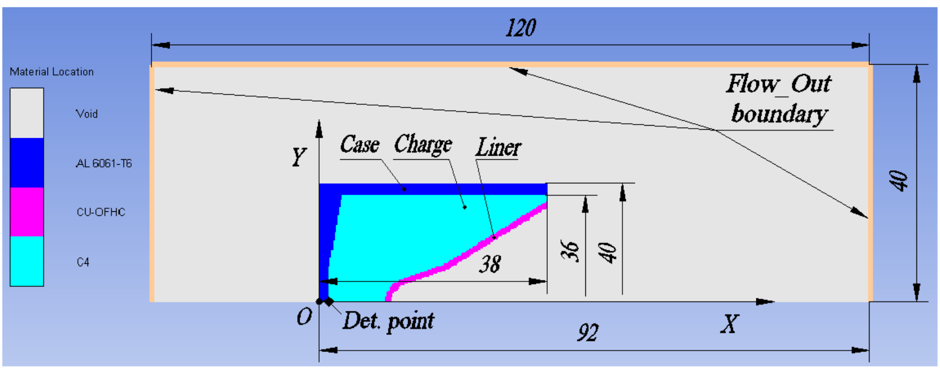

Fig. 3 Simulation model [mm]

Due to the axial symmetry of the shaped charge, the simulation model is constructed in the XOY coordinate system, where the origin O is at the center of the base of the case and the OX axis coincides with the axis of the shaped charge. The multi-material Euler – 2D solver is used to simulate the propagation process of the detonation wave and the jet formation [19]. All simulations were set up in the same way, including the following:

- The boundary region is 120 mm in the OX direction and a size of 40 mm in the OY direction, as shown in Fig. 3.
- A square grid with dimensions of 0.5×0.5 mm is used in the computational region to reduce the simulation time. This grid size makes it easier to observe signs of breakup or necking.
- Flowout boundary condition is applied to the computational boundary region. The interaction of explosive products and the case at the boundary of the calculation area is not considered.
- The point detonation method is used with the initial detonation point at the center of the charge base.
- The simulation is stopped when the jet tip is 92 mm away from the origin O (equivalent to 1.5 times the charge diameter from the base of the liner). This distance is expected to be in the mid to late stages of jet formation, allowing for observing signs of breakup or necking.
- The materials of the shaped charge parts are selected from materials available in the software library including C4 explosive for the charge, CU-OFHC copper for the liner, and AL 6061-T6 aluminium for the case. The models and parameters of materials are shown below.

2.2 Material Model of Explosive Charge

The C4 explosive uses the JWL (Jones-Wilkins-Lee) equation of state to describe its properties. The JWL equation of state of the explosion product has the form [18]:

$$p = A\left(1-\frac{\omega}{R_1 v}\right)\mathrm{e}^{-R_1 v} + B\left(1-\frac{\omega}{R_2 v}\right)\mathrm{e}^{-R_2 v} + \frac{\omega E}{v} \tag{1}$$

where p is the pressure of explosive products; ω, A, B, R_1, and R_2 are the experimental coefficients; $v = \rho_0/\rho$ is the ratio of initial density to the density at the time of calculation, and E is the specific energy of the explosive.

Input parameters in AUTODYN for the JWL equation of state include: ρ_0, A, B, R_1, R_2, ω, E_{CJ} (C-J Energy per unit volume), P_{CJ} (C-J Pressure), and D_{CJ} (C-J Detonation velocity).

These parameters for C4 explosives are given in Tab. 1 [20].

Tab. 1 Parameters in the JWL equation of state of C4 explosive

ρ_0 [kg/m^3]	A [Mbar]	B [Mbar]	R_1	R_2	ω	E_{CJ} [MJ/m^3]	P_{CJ} [Mbar]	D_{CJ} [m/s]
1601	6.0977	0.1295	4.5	1.4	0.25	9000	0.28	8193

2.3 Material Model of Liner Shaped Charge

The material of the liner is CU-OFHC copper with a density of 8 930 kg/m^3, which is elastic but subject to shock and deformation at high velocity, so the shock equation of state and Steinberg-Guinan strength model are used.

The Rankine-Hugoniot equations for the shock jump conditions can be viewed as a relationship between each two variables from a set of variables ρ (density), p (pressure), e (energy), u_p (particle velocity), and U (shock velocity). In most solid materials and some liquids, U and u_p have the following relationship [18]:

$$U = C_0 + Su_p \tag{2}$$

where C_0 and S are coefficients.

The Mie-Gruneisen formula of the equation of state, based on the Rankine-Hugoniot condition of shock has the form:

$$p = p_H + \Gamma\rho\left(e - e_H\right) \tag{3}$$

where it is supposed that $\Gamma\rho$ is a constant, and

$$p_H = \frac{\rho_0 C_0^2 \mu\left(1+\mu\right)}{\left[1-\left(S-1\right)\mu\right]^2} \tag{4}$$

$$e_H = \frac{1}{2}\frac{p_H}{\rho_0}\frac{\mu}{1+\mu} \tag{5}$$

where Γ is the Gruneisen coefficient, p_H is the Hugoniot pressure, e_H is the Hugoniot energy, ρ_0 is the initial density, and $\mu = (\rho/\rho_0)-1$.

In the case of high shock strengths, the relationship between U and u_p follows a nonlinear law, especially for non-metallic materials. To cater to this nonlinearity in AUTODYN, two linear fits to the shock velocity-particle velocity relationship $U_1 = C_1 + S_1u_p$, and $U_2 = C_2 + S_2u_p$ are used:

- when the shock compressions are low, determined by $v > VB$, this relationship has the form: $U = U_1$,
- when the shock compressions are high, determined by $v \leq VE$, this relationship has the form: $U = U_2$,
- when $VE < v < VB$, this relationship has the form:

$$U = U_1 + \frac{\left(U_2 - U_1\right)\left(v - VB\right)}{VE - VB} \tag{6}$$

More details on the shock state equation are presented in [18]. In AUTODYN, the input parameters of the shock equation of state for the copper material CU-OFHC are given in Tab. 2.

Tab. 2 Shock state equation parameters of the liner [20]

ρ_0 [kg/m^3]	Γ	C_1 [m/s]	S_1
8930	2.02	3940	1.489

The Steinberg-Guinan strength model is represented through the system of equations [18]:

$$G = G_0\left[1 + \frac{G'_p}{G_0}\frac{p}{\eta^{1/3}} + \frac{G'_T}{G_0}\left(T - 300\right)\right] \tag{7}$$

$$Y = Y_0 \left[1 + \frac{Y'_{\mathrm{p}}}{Y} \frac{p}{\eta^{1/3}} + \frac{G'_{\mathrm{T}}}{G_0} (T - 300) \right] (1 + \beta \varepsilon)^n \tag{8}$$

$$Y_0 (1 + \beta \varepsilon)^n \leq Y_{\max} \tag{9}$$

where β, n are the material constants; ε is the effective plastic strain; G_0 and Y_0 are the shear modulus and yield stress at time T_0 = 300 K, p = 0, ε = 0; G and Y are the shear modulus and yield stress under dynamic load; η is the compression ratio, $\eta = 1/v$; p is the pressure, T is the temperature (degrees K); $G'_{\mathrm{p}}, G'_{\mathrm{T}}, Y'_{\mathrm{p}}$ are the derivatives of G and Y for p, T.

The strength model parameters of CU-OFHC material are given in Tab. 3 [20].

Tab. 3 Steinberg-Guinan strength model parameters of the liner

G_0 [Mbar]	Y_0 [Mbar]	$Y_{\max}$ [Mbar]	β	n	G'_{p}	G'_{T} [Mbar/K]	Y'_{T}	T_{melt} [K]
0.4770	0.0012	0.0064	36	0.45	1.35	-1.798×10^{-4}	0.003396	1 790

2.4 Material Model of the Shaped Charge Case

The case material is AL 6061-T6 aluminium with a density of 2 703 kg/m^3. When subjected to explosive loading, the material undergoes large deformation, leading to changes in both the volume and shape of the element. Therefore, we use the shock equation of state and the Steinberg-Guinan strength model to describe the material model of the case.

The input parameters in AUTODYN of the shock equation of state for material AL 6061-T6 are given in Tab. 4 [20].

Tab. 4 Shock state equation parameters of the case

ρ_0 [kg/m^3]	Γ	C_1 [m/s]	S_1
2 703	1.97	5 240	1.4

The strength model parameters of AL 6061-T6 material are given in Tab. 5 [20].

3 Simulation Results and Discussion

3.1 Influence of Apex Angle and Base Angle of Liner on the Jet Characteristics

The double cone liner is designed with dimensions D = 34 mm, δ = 1 mm, r = 3 mm, and h_1 = 10.2 mm (h_1/D = 0.3). When studying the effect of the apex angle, the base angle was fixed at 60°, and the apex angles varied with the dimensions of 32°, 40°, 46°, 50°, and 56°. When studying the effect of the base angle, the apex angle was fixed at 40°, and the base angles were selected to be 46°, 50°, 56°, 60°, and 70°. The selection of these angles was predicted to create clearer observations of the simulation results.

Tab. 5 Steinberg-Guinan strength model parameters of the case

G_0 [Mbar]	Y_0 [Mbar]	Y_{max} [Mbar]	β	n	G'_p	G'_T [Mbar/K]	Y'_T	T_{melt} [K]
0.2760	0.0029	0.0068	125	0.1	1.8	-1.700×10^{-4}	0.018908	1 220

Simulation results of the influence of different apex angles on jet characteristics are shown in Fig. 4 and Tab. 6. When the apex angle increases from 32° to 56°, jet characteristics change insignificantly. The jet tip velocity decreases from 4 790 m/s to 4 551 m/s, corresponding to a 4.99 % reduction, while the jet tail velocity increases from 1 639 m/s to 1 762 m/s, corresponding to a 7.51 % increase. The velocity difference between the tip and tail of the jet is the largest at an angle of 32°, and this difference gradually decreases as the apex angle increases to 56° (a reduction of 11.48 %). This leads to a reduction in jet elongation and a 4.56 % decrease in jet length, from 39.5 mm to 37.7 mm. The simulation results also show that, at an apex angle of 40°, the jet velocity is 4 755 m/s, and the jet length is 39.2 mm, which are slightly lower compared to the apex angle of 32° with corresponding values of 4 790 m/s and 39.5 mm. However, at the apex angle of 32°, the jet shows signs of breakup (position A in Fig. 5), whereas, at the apex angle of 40°, the jet is more continuous and stable, which is likely to result in better penetration performance.

The influence of different base angles on jet characteristics is clearly illustrated in Fig. 6, where the velocity gradient shows a significant variation as the base angle increases from 46° to 70°.

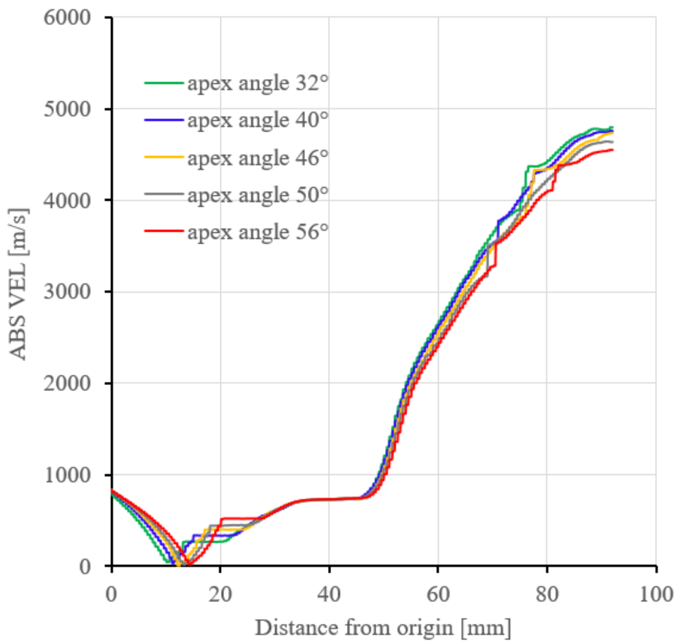

Fig. 4 Jet velocity gradient for different apex angles

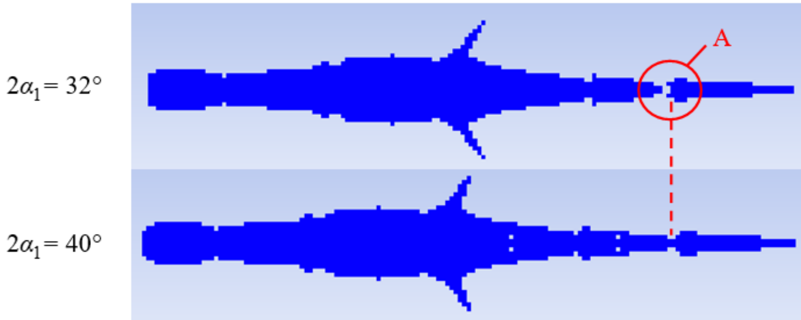

Fig. 5 Jet shape with apex angle 32° *and* 40°

Tab. 6 Jet characteristics with different apex angles

Apex angle	Jet tip velocity V_{tip} [m/s]	Jet tail velocity V_{tail} [m/s]	$V_{tip} - V_{tail}$ [m/s]	Jet length [mm]
32°	4 790	1 639	3 151	39.5
40°	4 755	1 692	3 063	39.2
46°	4 732	1 721	3 011	38.6
50°	4 634	1 751	2 883	38.2
56°	4 551	1 762	2 789	37.7

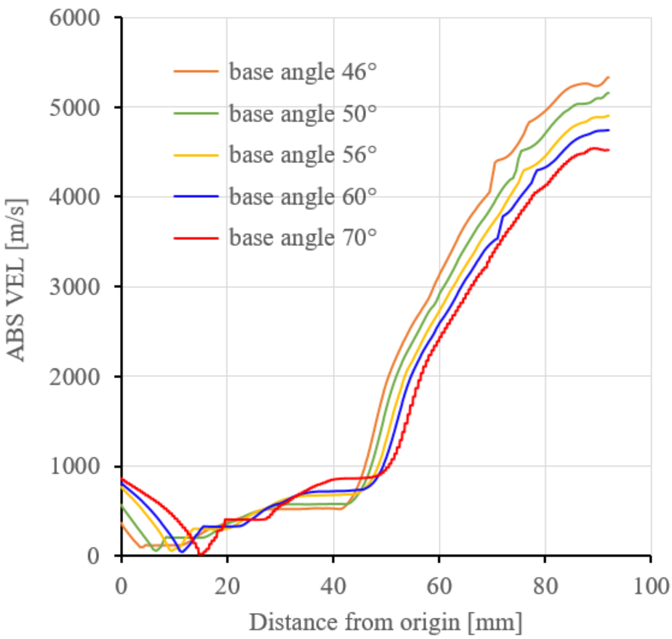

Fig. 6. Jet velocity gradient for different base angles

Tab. 7 presents the jet characteristics at various base angles. At a base angle of 46°, the jet characteristics parameters are the largest and then gradually decrease when the base angle increases to 70°, in which the jet tip velocity decreases by 15.14 %, the velocity difference decreases by 19.3 % and the jet length decreases by 12.94 %. At a base angle of 70°, the jet parameters are significantly lower compared to other base angles, suggesting that the jet penetration capability at this base angle is likely to be low. For base angles of 46°, 50°, and 56°, the jet characteristics parameters show relatively good values. However, at these angles, the jet exhibits an earlier necking phenomenon compared to the jet at a 60° base angle (positions B, C, D, E in Fig. 7). This indicates that the material flow density distribution of the jet formed at a 60° base angle is more balanced, ensuring better stability and performance of the jet.

Tab. 7 Jet characteristics with different base angles

Base angle	Jet tip velocity V_{tip} [m/s]	Jet tail velocity V_{tail} [m/s]	$V_{\text{tip}} - V_{\text{tail}}$ [m/s]	Jet length [mm]
46°	5 334	1 807	3 527	42.5
50°	5 153	1 725	3 428	41.7
56°	4 897	1 671	3 226	40.2
60°	4 755	1 692	3 063	39.2
70°	4 525	1 679	2 846	37.0

3.2 Influence of Cone Angle Transition Position on the Jet Characteristics

The double cone liner is designed with the following dimensions: $D = 34$ mm, $\delta = 1$ mm, $r = 3$ mm, $2\alpha_1 = 40°$; $2\alpha_2 = 60°$. Simulation will be conducted for different transition positions of the cone angle at 6.8 mm, 10.2 mm, 13.6 mm, 17.0 mm, and 20.4 mm, corresponding to transition position ratios of 0.2, 0.3, 0.4, 0.5, and 0.6 relative to the shaped charge base diameter. The simulation results of the influence of cone angle transition position on the jet characteristics are shown in Fig. 8 and Tab. 8. At a cone angle transition position $h_1/D = 0.2$, the jet tip velocity and velocity difference have the lowest values, leading to a limited jet elongation capability, with the jet length reaching only 38.6 mm. When the cone angle transition position increases from $h_1/D = 0.2$ to $h_1/D = 0.6$, the tip velocity and velocity difference increase sharply by 25.8 % and 33.7 %, respectively. However, the jet length shows only a modest improvement, increasing by 5.18 %. In addition, at positions h_1/D greater than 0.3, the jet diameter is smaller than at position $h_1/D = 0.3$ (Tab. 8). Moreover, at positions $h_1/D = 0.5$ and $h_1/D = 0.6$, signs of necking appear earlier (positions G, H compared to F in Fig. 9), indicating a potential decrease in jet density, which would lead to a reduction in the jet penetration ability.

Based on the above results and observations, it can be inferred that at the transition position of h_1/D between 0.3 and 0.4, the jet is predicted to have the best penetration capability. Another important note is that with the proposed design model, as the h_1 length increases, the total height of the liner also increases, reducing the space between the base of the charge and the top of the liner. This reduction may pose difficulties in arranging a booster (when necessary) or potentially in altering the overall structure of the projectile. Therefore, a transition cone angle position value of h_1/D around 0.3 is deemed appropriate for this shaped charge model.

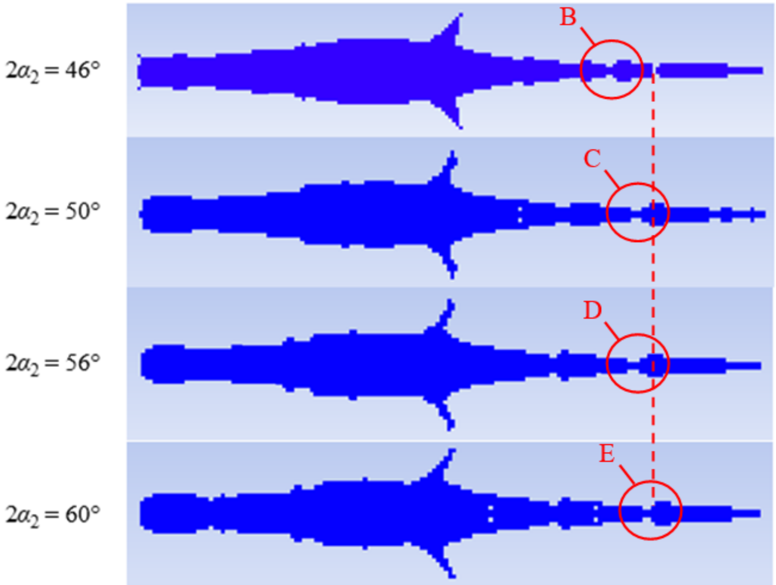

Fig. 7 Jet shape with base angles 46°, 50°, 56°, 60°

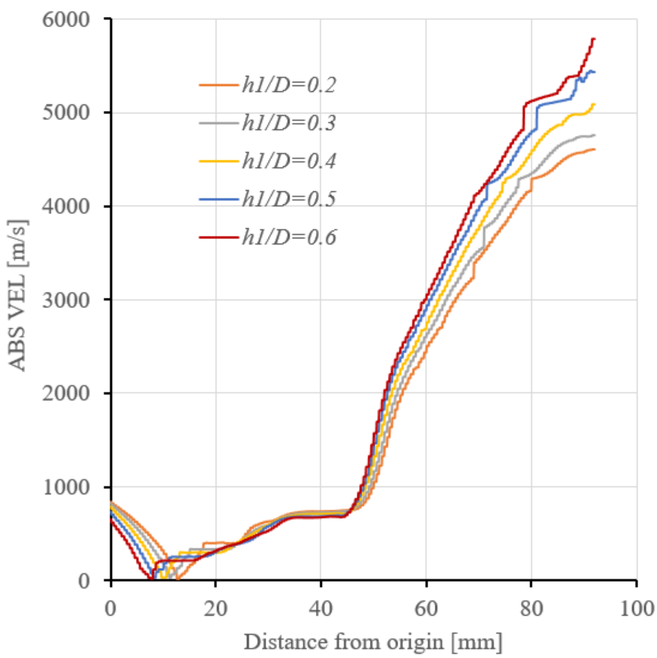

Fig. 8 Jet velocity gradient with different angular change positions

Tab. 8 Jet characteristics with different h_1/D

h_1/D	Jet tip velocity V_{tip} [m/s]	Jet tail velocity V_{tail} [m/s]	$V_{tip} - V_{tail}$ [m/s]	Jet length [mm]	Jet diameter [mm]
0.2	4 600	1 631	2 969	38.6	3.0
0.3	4 755	1 692	3 063	39.2	3.0
0.4	5 088	1 766	3 322	39.8	2.9
0.5	5 438	1 828	3 610	40.2	2.9
0.6	5 788	1 817	3 971	40.6	2.6

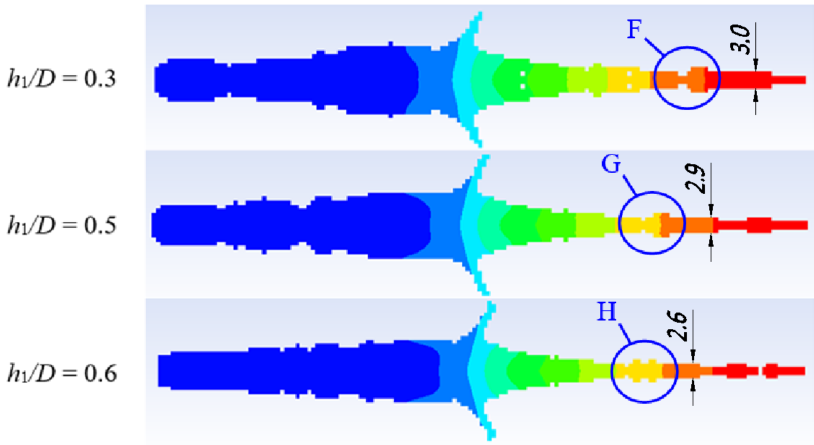

Fig. 9 Jet velocity state with different h_1/D

4 Conclusion

In this paper, the influence of several dimensional parameters of the double cone liner shape, including apex angle, base angle, and cone transition position, on the jet characteristics was investigated, and the conclusions are drawn as follows.

ANSYS AUTODYN software is a powerful and advanced numerical simulation tool, that can be effectively applied to study the jet formation of shaped charges. Simulations on the ANSYS AUTODYN 2D platform on the changes of the dimensions of the apex angle, base angle, and cone angle transition position to the jet formation process have been successfully performed, providing a visual understanding of the jet formation process.

The simulation results were analyzed and discussed, demonstrating that certain jet characteristics are significantly improved when the apex and base angles have small values and the cone angle transition position from the top of the liner has large values.

The shaped charge model used in this study features a double cone liner with an apex angle of approximately 40°, a base angle of about 60°, and a cone transition position located at 0.3 times the liner's base diameter from the top. These shape parameters are predicted to optimize jet penetration performance, making them a promising design choice for enhancing the effectiveness of shaped charges.

The findings of this study serve as a useful reference for designing the shape parameters of double-cone liners for small-sized shaped charges, particularly for the proposed shaped charge model, to improve jet performance.

References

[1] WALTERS, W.P. and J. ZUKAS. *Fundamentals of Shaped Charge*. New York: Wiley Interscience Publication, 1989. ISBN 978-0-471-62172-0.

[2] SIMON, J. *The Effect of Explosive Detonation Characteristics on Shaped Charge Performance* [online]. Maryland: Ballistic Research Laboratories Aberdeen Proving Ground, 1974 [viewed 2024-02-23]. Available from: https://apps.dtic.mil/sti/pdfs/AD0785680.pdf

[3] ELSHENAWY, T., G.M. ABDO and A. ELBEIH. Effect of Explosives Charges Types on the Jet Characteristics, Penetration Performance and Patterns of Shaped Charges. *Scientific Reports*, 2024, **14**, 26282. DOI 10.1038/s41598-024-75727-0.

[4] NAN, Y.X., J. JIANG, S. WANG, J.B. MEN and D.P. CHEN. Penetration Capability of Shaped Charge Loaded with Different High-Energy Explosives. In: *28th International Symposium on Ballistics*. Atlanta, 2014, pp.1039-1044. ISBN: 978-1-60595-149-2.

[5] WANG, Z., J.W. JIANG, S.Y. WANG and H. LIU. Jet Formation and Penetration Study of Double-Layer Shaped Charge [online]. *Journal of Energetic Materials,* 2017, **36**(2), pp. 152-168 [viewed 2024-12-12]. DOI 10.1080/07370652.2017.1326987.

[6] MINH DO, V., M. THAI LE, X. SON BUI, H. NGUYEN PHAM and P. LINH NGUYEN. Influence of Wave Shaper Position on Jet Formation and Penetration Depth. *Advances in Military Technology***,** 2020**,** **15**(1), pp. 355-364. DOI 10.3849/aimt.01385.

[7] LIANG, Z, J. JIN, X. GUO and Q. QI. Numerical Simulation of the Effect of Conical-Disc Wave-Shaper on Jet Performance. In: *2024 2nd International Conference on Signal Processing and Intelligent Computing*. Guangzhou: IEEE, 2024. DOI 10.1109/SPIC62469.2024.10691582.

[8] HELD, M. Liners for Shaped Charges [online]. *Journal of Battlefield Technology* 2001, **4**(3) [viewed 2024-12-18]. Available from: https://cdn.preterhuman.net/texts/terrorism_and_pyrotechnics/explosives/Shaped_Charges_Penetrators/Liners%20for%20Shaped%20Charges%20by%20Manfred%20Held%20(2001).pdf

[9] BOURNE, B., K.G. COWAN and J.P. CURTIS. Shaped Charge Warheads Containing Low Melt Energy Metal Liners. In: *Proceedings of the 19th International Symposium on Ballistics* [online]. 2001, pp. 583-590 [viewed 2024-12-18]. Available from: http://www.ciar.org/ttk/mbt/papers/symp_19/WM05_583.pdf

[10] WANG, T.F. and H.R. ZHU. Copper-Tungsten Shaped Charge Liner and its Jet. *Propellants, Explosives, Pyrotechnics*, 1996, **21**(4), pp. 193-195. DOI 10.1002/prep.19960210406.

[11] SADRI SEN, I. and A. GOKHAN. An Application of Explosive Metal Forming in Military Field: The Relationship Between Shaped Charge Jet Formation and Thickness Variation Along Liner Length of Conical Copper Liner. *Arabian Journal for Science and Engineering*, 2013, **38**(12), pp. 3551-3562. DOI 10.1007/s13369-013-0642-x.

[12] KANG, Y. and J. JEON. Finite Element Analysis of the Impact of Liner Thickness and Hydrodynamic Limit on the Penetration Depth of a Shaped Charge Warhead. *Journal of Mechanical Science and Technology*, 2018. **32**(12), pp. 5797-5805. DOI 10.1007/s12206-018-1127-3.

[13] HONG, B., W. LI, Y. LI, Z. GUO and B. YAN. Jet Formation and Penetration Performance of a Double-layer Charge Liner with Chemically-Deposited Tungsten as the Inner Liner. *Defence Technology*, 2024, **33**, pp. 374-385. DOI 10.1016/j.dt.2023.08.016.

[14] COMBRINCK, M.L., T. GADAL, A. HARGREAVES and J.E. MARTIN. Velocity Tracking of Shaped Charge Wire Formation and Propagation Towards the Target. *Journal of Energetic Materials*, 2024, **42**(3), pp. 362-381. DOI 10.1080/07370652.2022.2079772.

[15] KEMMOUKHE, H., S. SAVIĆ, S. TERZIĆ, M. LISOV, N. REZGUI and H. SEDRA. Improvement of the Shaped Charge Jet Penetration Capability by Modifying the Liner Form Using AUTODYN-2D. *Scientific Technical Review*, 2019, **69**(1), pp. 10-15. DOI 10.5937/str1901010K.

[16] SAYED, E.E.E., T.A. ELSHENAWY, M.A. SHAKER and A.M. RIAD. Influence of Different Shaped Charge Parameters on Jet Penetration into Metallic Target. *Journal of Physics: Conference Series*, 2022, **2299**, 012016. DOI 10.1088/1742-6596/2299/1/012016.

[17] LI, H., P. LI, H. DUAN and Z. ZHANG. Study on the Jet Formation and Penetration Performance of Shaped Charge with Untypical Double-Cone Titanium Liner. *Journal of Physics: Conference Series*. 2023, **2599**(1), 012028. DOI 10.1088/1742-6596/2599/1/012028.

[18] *AUTODYN Theory Manual* [online]. 2005 [viewed 2024-11-12]. Available from: https://fr.scribd.com/document/493503559/Autodyn-Theory-Manual

[19] GÜREL, E. *Modeling and Simulation of Shaped Charges*. [Master’s Thesis] [online]. Ankara: Middle East Technical University 2009 [viewed 2024-11-12]. Available from: https://etd.lib.metu.edu.tr/upload/12610830/index.pdf

[20] *ANSYS Autodyn User’s Manual* [online]. 2018 [viewed 2024-12-12]. Available from: https://fr.scribd.com/document/453341462/ANSYS-Autodyn-Users-Manual-pdf